Modeling the Dynamics of Cancer Growth and Treatment

Michael Barmann, Ryan Wilson, Nicolas Malloy,
Andrew Xiang, Junsang You

MS Applied Mathematics Project 2018-2019

Department of Mathematics and Statistics
The University of Massachusetts Amherst
May 9, 2019

Abstract

In this project, we investigate the dynamics of cancer growth and treatment using a combination of statistical, analytical, and numerical approaches. We first review three common models of cancer growth–the Exponential, Power Law, and Gompertz-Laird models–and then fit these models to tumor volume data collected from laboratory mice. We obtain parameter estimates and assess how well each model fits the data. We also employ a Support Vector Regression (SVR) algorithm to predict growth trends based on the given data. Finally, we examine a treatment model adapted from the competitive two-equation Lotka-Volterra system, and perform a stability analysis and obtain numerical results.

Contents

1 Introduction **1**

2 Basic Growth Models **2**
2.1 The Exponential Model 2
2.2 The Power Law Model 2
2.3 The Gompertz-Laird Model 3

3 Data and Model Fits **4**
3.1 Summary of Mouse Data 4
3.2 Parameter Results 4
3.3 Model Fits 5
3.4 Assessing Predictive Ability 6
3.5 A Support Vector Regression Model 7

4 Two-Strain Competition Models **9**
4.1 The Competitive Lotka-Volterra Equations 9
4.2 A Two-Strain Treatment Model 11

5 Conclusion **15**

1 Introduction

According to this year's annual report by the American Cancer Society, more than 1.7 million Americans will receive a cancer diagnosis in 2019, and more than 600 thousand Americans will die from the disease [4]. What's more, the National Cancer Institute now projects that more than 38 percent of the world's population will at receive a cancer diagnosis "at some point in their lifetimes" [1]. These statistics lay bare the scale of the devastation that cancer continues to inflict on our society, on both a national and global scale. In the last several decades, scientists have made great strides in understanding the biological mechanisms of the disease, leading to improved diagnostic capabilities and chemo- and immunotherapy treatments. However, despite much scientific progress, the 5-year survival rates for many cancers, such as pancreatic, colorectal, and liver cancers, have been only marginally improved in the last several decades [1]. Clearly, the disease remains a major public health issue, and necessitates continued study and medical innovation.

At the biological level, cancer refers to a diverse family of diseases sharing a common genesis–the uncontrolled growth of cells, arising from a breakdown in the homeostatic signaling that governs cell division. Mathematical biology offers a promising approach to predicting the dynamics of this faulty cell growth, with goal of furnishing insight into potential treatments.

Given the complexity of the disease, approaches to modeling cancer are numerous and highly varied. In this paper, we opt for a combination of statistical, machine learning, and differential equation methods to analyze tumor growth in laboratory mice. We begin by reviewing the Exponential, Power Law, and Gompertz-Laird models of tumor growth. We then fit tumor volume data collected from mice to each model, obtain parameter estimates, and assess each model's predictive power. Next, we employ a Support Vector Regression (SVR) algorithm to predict the growth trends in the mice data. We then review the competitive Lotka-Volterra equations in the context cancer modeling, and present a treatment model for tumor growth which is adapted from the Lotka-Volterra model. Finally, we conclude with a discussion of our results and discuss some of the implications for oncology.

2 Basic Growth Models

2.1 The Exponential Model

The Exponential model is perhaps the simplest model that is used to study cellular growth. The model is given by

$$\frac{dv}{dt} = \alpha t, \qquad \alpha > 0$$

where $v(t)$ denotes the volume of cancer cells in cubic millimeters at time t, and $\alpha > 0$ is the per capita growth rate of the cancer cells. This very simple ODE has solution

$$v(t) = v_0 e^{\alpha t},$$

where $v_0 = v(t = 0)$ denotes the initial tumor volume. In this paper, we are interested in macroscopic tumor growth, so it suffices to pick an initial value v_0 which is $O(1)$. For simplicity, we take $v_0 = 1$ mm^3. The Exponential model assumes a growth rate which remains proportional to the volume of the tumor, and hence predicts unbounded growth. While this model has been shown to accurately describe the growth of bacteria in vitro over a period of days, this model is generally not valid for modeling longterm growth [2].

2.2 The Power Law Model

The Power Law growth model is given by

$$\frac{dv}{dt} = \alpha v^{\beta},$$

where $\alpha > 0$ is the per capita growth rate, and $\beta > 0$ is a dimensionless constant. The Power Law growth model is a generalization of the Exponential model in which the tumor growth rate is assumed to be proportional to the tumor volume raised to a power $\beta > 0$ (usually $\beta \leq 1$). An allometric scaling argument has been put forth for choosing $\beta = 2/3$ based upon the idea that the ratio of a tumor's surface area to volume v is roughly proportional to $v^{2/3}$ if the tumor is thought of as a sphere [7]. The solution to the model is

$$v(t) = \left[\alpha(1-\beta)t + v_0^{1-\beta}\right]^{\frac{1}{1-\beta}}.$$

Again, we take $v_0 = 1$ mm^3, simplifying the equation to

$$v(t) = \left[\alpha(1-\beta)t + 1\right]^{\frac{1}{1-\beta}}.$$

The benefit of the Power Law and Exponential models is their simplicity, but they share the characteristic that $v \to \infty$ as $t \to \infty$, which is of course not biologically realistic. Hence, we shall consider a third model which contains a horizontal asymptote.

2.3 The Gompertz-Laird Model

The third equation we consider is the Gompertz-Laird equation, originally put forth by A.K. Laird in 1974 [5]:

$$\frac{dv}{dt} = v(\alpha - \beta \ln v).$$

The solution to this nonlinear ODE yields the following sigmoidal curve:

$$v(t) = v_0 \exp\left[\frac{\alpha}{\beta}\big(1 - \exp(-\beta t)\big)\right].$$

Again, we take $v_0 = 1$ mm^3, giving the slightly simpler equation $v(t) = \exp\left[\frac{\alpha}{\beta}(1 - \exp(-\beta t)\right]$. An important difference of the Gompertz-Laird equation is that it approaches a limiting value. Indeed,

$$\lim_{t\to\infty} \exp\left[\frac{\alpha}{\beta}\big(1 - \exp(-\beta t)\big)\right] = \exp\left(\frac{\alpha}{\beta}\right).$$

The parameters α and β lack a clear biological interpretation, but its clear that both influence the shape and upper asymptote of the sigmoidal curve. These parameters also both determine the inflection point, which occurs when

$$t = -\frac{1}{\beta} \ln\left(\frac{\beta}{\alpha}\right),$$

at which time we have $v(t) = e^{\alpha/\beta - 1}$. The Gompertz equation and its variants, including the

Gompertz-Laird equation, have a rich history in the use of population modeling, especially in modeling cancer growth in mice [5]. Given the extensive usage of the Gompertz equation in the biological literature, we expect this model to exhibit the best fit for our data set.

3 Data and Model Fits

3.1 Summary of Mouse Data

The data used to fit the models consists of ten mice that had Murine Lewis lung carcinoma. Their tumor growth was measured at various intervals for about 20 days beginning five days after the mice were infected with the cancer. The plot below shows the tumor volume measurements for each mouse over the course of the study.

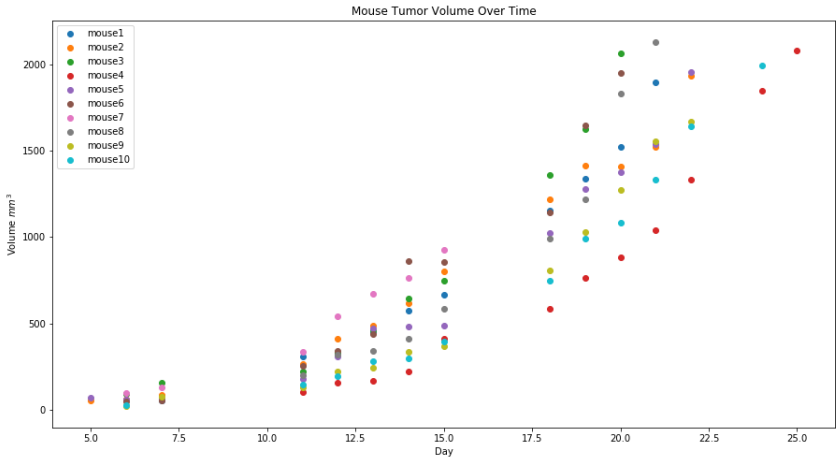

Fig 1: Mice tumor volume data collected over 20 days.

3.2 Parameter Results

We took an individual approach to estimating the parameters, thinking of each mouse as a realization of the tumor growth process. Using the method of maximum likelihood with normally distributed errors [3], we obtained three sets of parameter estimates for each mice (one set for each model). The true parameter estimates for each model were taken to be the mean of the ten corresponding estimates. The results of the parameter fitting and the associated standard errors are given in the table below.

Model	Mean α	Std Error α	Mean β	Std Error β
Exponential	0.3776	0.0127	-	-
Power Law	1.08623117	0.10323831	0.75070674	0.02249964
Gompertz	0.77146321	0.03791247	0.08738799	0.00800713

Fig 2: Parameter Fitting Results

3.3 Model Fits

We first assess the fit of the exponential model. If the tumor volume does in fact obey the Exponential growth model, then the natural logarithm of the tumor volume should be linear with respect to time. The log plots for all ten mice are given below.

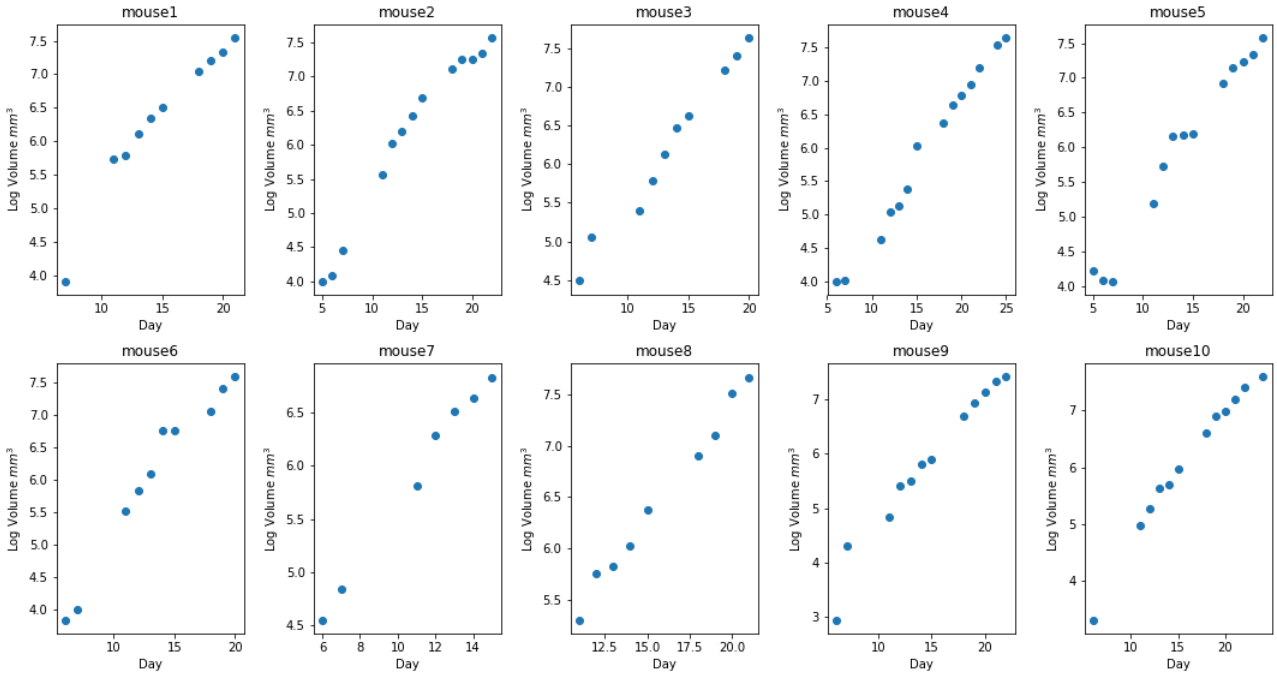

Fig 3: Log v versus t plots for each individual.

The log plots above show an approximately linear relationship, but the fit is not perfect. In particular, the log plots for Mice 1,3,5 and 9 clearly do not exhibit a linear fit.

We then used three different metrics to assess each model: the sum of the squared errors (SSE), the Bayesian information criterion (BIC), and Akaike information criterion (AIC). The equations for these metrics are given below.

$$SSE = \sum (y_i - \hat{y}_i)^2,$$

$$AIC = n \log\left(\frac{SSE}{n}\right) + 2p$$

$$BIC = n \log\left(\frac{SSE}{n}\right) + p \log(n)$$

In the above equations, the y_i's are the actual values, the $\hat{y}_i$'s are the predicted values, n is the number of data points, and p is the number of parameters in the model.

Model	Mean SSE	Mean AIC	Mean BIC
Exponential	79.00	20.64	21.02
Power Law	0.67	-33.69	-32.93
Gompertz	1.40	-28.61	-27.85

Fig 4: Goodness of fit results.

For all three metrics, the lower the number the better the fit. We see that the Power Law model had the best fit by all three metrics, whereas the Exponential model had the poorest fit across all three metrics.

3.4 Assessing Predictive Ability

We also tested the predictive ability of each model. To do this we computed parameter estimates based on the first six data points for each mouse, and then used these parameters to predict the remaining points. We used the root mean squared error (RMSE) as our metric for assessing the accuracy of the predicted data, which is calculated by the following formula:

$$\text{RMSE} = \sqrt{\frac{\sum (y_i - \hat{y}_i)^2}{n}}$$

The results are summarized in the figures below.

Metric	Power Law	Gompertz	Exponential	SVR
Mean RMSE	303.03	451.17	7426.66	361.93

Fig 5: Predictive Ability based on the RMSE.

The results in table above show that the Power Law predicted the latter four data points with the highest accuracy. This result is in agreement with our earlier finding that the Power

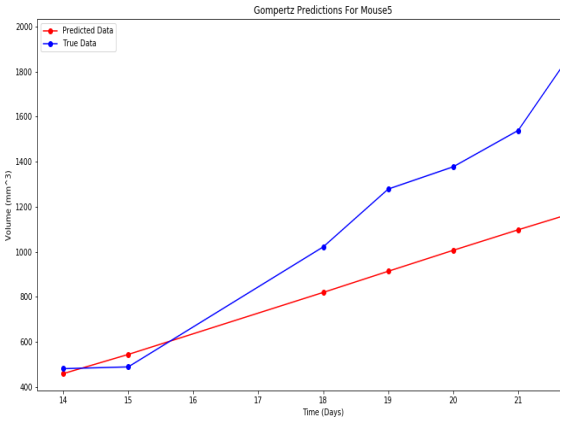

Fig 6a: Gompertz-Laird Predictions

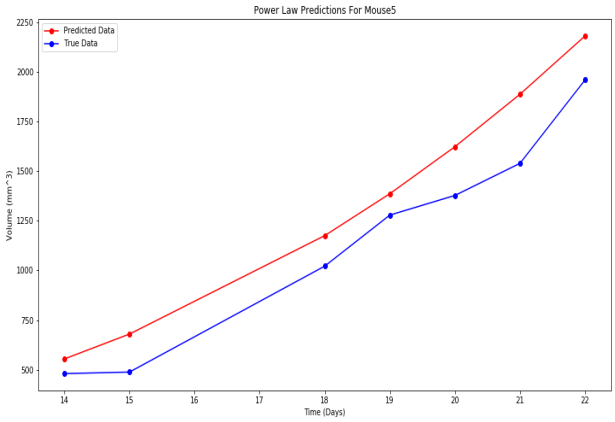

Fib 6b: Power Law Predictions

Law fit all ten data points the best. We believe, however, that the Gompertz model would exhibit the best fit if the data was taken over a longer period of time, as the growth rate of the tumor should eventually slow down.

3.5 A Support Vector Regression Model

We also constructed a model using a more advanced technique: Support Vector Machine Regression (SVR). Normally, SVR is used with data sets much larger than ours, but we feel it is a useful test of how a more sophisticated method fairs against the simpler parameter-fitting approaches. The performance of SVR is heavily influenced by the chosen hyperparameters and the kernel used. We chose the Radial Basis Function (RBF) as our kernel, which has the form

$$K(x, x') = \exp(-\gamma||x - x'||).$$

This model has two hyperparameters γ and c. The first parameter γ controls a constant in the RBF kernel's computation of distance between two points. The smaller γ is, the smaller the penalty for being farther apart. The second parameter c determines a threshold for the maximum leniency before very incorrect predictions are penalized. We selected values of $c = 10^3$ and $\gamma = 10^{-5}$ as our hyperparameters. The SVR's performance on the data set for each mouse can be seen in figures below. The blue lines indicate the true tumor data and the red lines indicate the SVR's predictions.

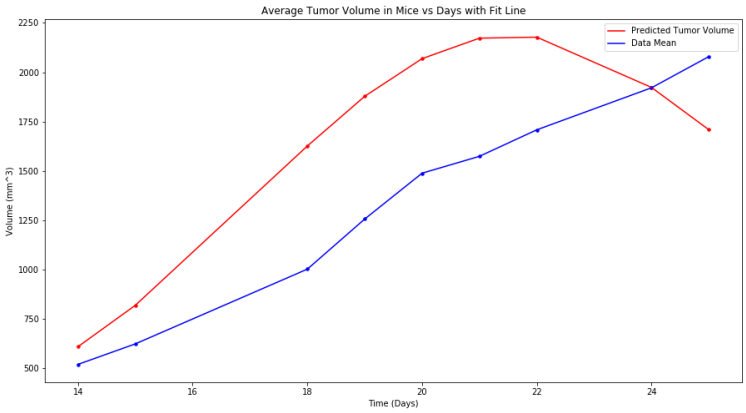

Fig 7: SVR model predictions versus the actual data.

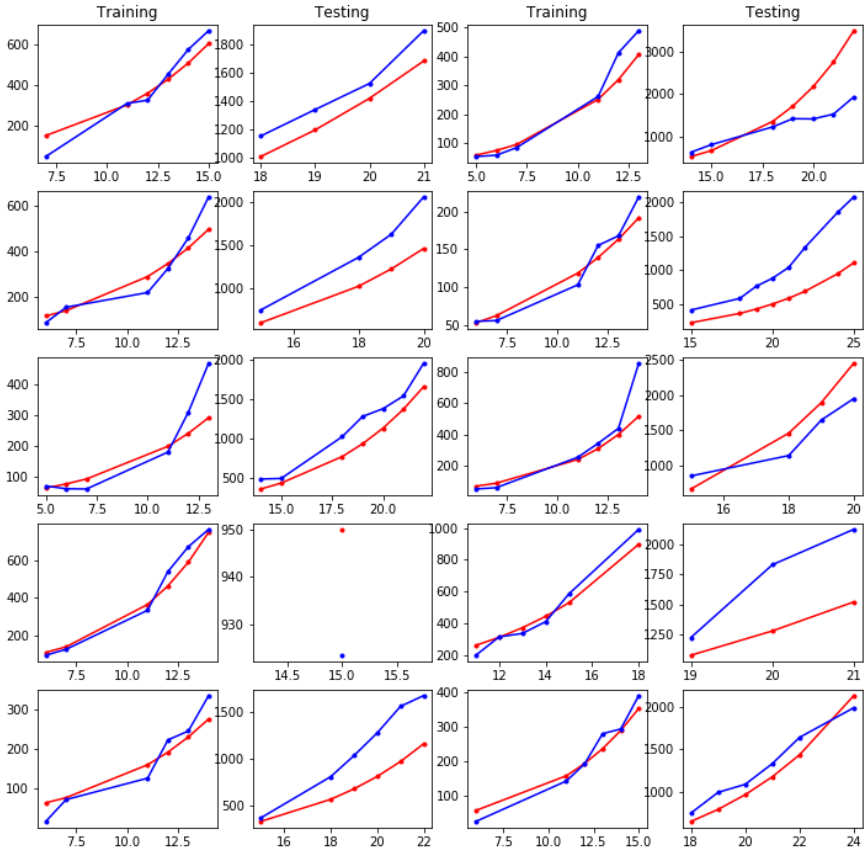

Fig 8: SVM training and testing data for each individual.

It's clear from the plots above that the SVR model exhibited relatively poor predictive ability for the average tumor volume over the last 11 days of the measurement period. Of course, this is not surprising given the extremely small number of data points used. Looking at the individual plots, the SVR model performed modestly well on Mice 1,5,6, and 10, but had poor performance on the remaining mice. Again, a paucity of data was clearly the major limiting factor in the accuracy of the model. In particular, Mouse 7 only had a single data

point beyond day 14 on which the SVR model made a prediction.

4 Two-Strain Competition Models

In the previous sections, we took a statistical approach to analyzing tumor growth based on single equation models. In this section, we consider a different approach based on the stability analysis of systems of differential equations. We begin by reviewing one of the most commonly used family of models in population biology: the competitive Lotka-Volterra equations.

The competitive Lotka-Volterra equations are used to model the dynamics of competing populations at both the micro and macroscopic level ("competition" in this case generally refers to vying for shared resources such as food, water, space, and/or predation) [6]. The general form for the N-species competition model is given by

$$\frac{dx_i}{dt} = r_i x_i \left(1 - \frac{\sum_{j=1}^{N} \alpha_{ij} x_j}{K_i}\right), \qquad i = 1, 2, \ldots, N.$$

where $x_i = x_i(t)$ denotes the population of species x_i at time t. The parameters of this model are r_i, which is the per capita growth rate of species i, and K_i, the carrying capacity of species i, and α_{ij}, the "competitive effect" of species j on species i. This model assumes that in the absence of competition, each species will exhibit logistic growth and tend towards its carrying capacity as $t \to \infty$. We now review the possible dynamics for the $N = 2$ case before introducing our adapation of this model.

4.1 The Competitive Lotka-Volterra Equations

Cancer cells and healthy cells can be thought of as two species in competition for space, oxygen, and nutrients. Letting $x = x(t)$ represent the volume of healthy cells at time t, and letting $y = y(t)$ represent the volume of tumor cells at time t, the competitive Lotka-Volterra model is

$$\frac{dx}{dt} = r_x x \left(1 - \frac{x}{K_1}\right) - b_1 xy$$

$$\frac{dy}{dt} = r_y y\left(1 - \frac{y}{K_2}\right) - b_2 xy,$$

where all of the constants are assumed to be positive. To simply calculations, the model is non-dimensionalized using the following change of variables: $\tau = r_x t,\ M = x/K_1,\ N = y/K_2$. The dimensionless equations are then given by

$$\frac{dM}{d\tau} = M(1 - M - \beta_1 N)$$
$$\frac{dN}{d\tau} = \rho N(1 - N - \beta_2 M)$$

where $\rho := r_y/r_x$, $\beta_1 := b_1 K_2/r_x$ and $\beta_2 := b_2 K_1/r_y$ are positive dimensionless constants. This system has four fixed points: $(M^*, N^*) = (0,0), (1,0), (0,1), (\frac{\beta_1 - 1}{\beta_1\beta_2 - 1}, \frac{\beta_2 - 1}{\beta_1\beta_2 - 1})$. The first fixed point $(0,0)$ corresponds to the mutual extinction of both populations. The second fixed point $(1,0)$ corresponds to the case where the tumor cells are extinct and the healthy cell population is at its carrying capacity, and the third fixed point $(0,1)$ corresponds to the reverse scenario. The fourth fixed point corresponds to the case where the healthy and cancerous cells co-exist, and is hence termed the "coexistence fixed point". A stability analysis is used to analyze the dynamics for the four main scenarios. The Jacobian matrix evaluated at the generic fixed point (M^*, N^*) is given by

$$J_{(M^*,N^*)} = \begin{pmatrix} 1 - 2M^* - \beta_1 N^* & -\beta_1 M^* \\ -\rho\beta_2 N^* & \rho(1 - 2N^* - \beta_2 M^*) \end{pmatrix}.$$

Evaluating the Jacobian at the first three fixed-points:

$$J_{(0,0)} = \begin{pmatrix} 1 & 0 \\ 0 & \rho \end{pmatrix}, \quad J_{(1,0)} = \begin{pmatrix} -1 & -\beta_1 \\ 0 & \rho(1 - \beta_2) \end{pmatrix}, \quad J_{(0,1)} = \begin{pmatrix} 1 - \beta_1 & 0 \\ -\rho\beta_2 & -\rho \end{pmatrix}.$$

And the Jacobian evaluated at the coexistence fixed point, which we denote by (M_c^*, N_c^*) comes out to

$$J_{(M_c^*,N_c^*)} = \begin{pmatrix} \frac{1-\beta_1}{\beta_1\beta_2 - 1} & \frac{\beta_1(1-\beta_1)}{\beta_1\beta_2 - 1} \\ \frac{\rho\beta_2(1-\beta_2)}{\beta_1\beta_2 - 1} & \frac{\rho(1-\beta_2)}{\beta_1\beta_2 - 1} \end{pmatrix}.$$

The Jacobian eigenvalues for the first three fixed-points are as follows:

$$(0,0): \ \lambda_1 = 1, \lambda_2 = \rho$$
$$(1,0): \ \lambda_1 = -1, \lambda_2 = \rho(1-\beta_2)$$
$$(0,1): \ \lambda_1 = 1-\beta_1, \lambda_2 = -\rho.$$

Since we are only interested in the cases where the coexistence fixed point to lies in the first quadrant (since population values must be nonnegative), we must have either $\beta_1\beta_2 < 1$ or $\beta_1\beta_2 > 1$. This gives rise to four different cases: $\beta_1, \beta_2 > 1$ (case 1), $\beta_1 > 1$ and $\beta_2 < 1$ (case 2), $\beta_1 < 1$ and $\beta_2 > 1$ (case 3), and $\beta_1, \beta_2 < 1$ (case 4). We begin by noting that in all cases, $(0,0)$ is a repeller because the Jacobian eigenvalues 1 and ρ are always positive. If $\beta_1, \beta_2 > 1$, then the Jacobian eigenvalues of $(1,0)$ and $(0,1)$ are all negative, and so $(1,0)$ and $(0,1)$ are both attractors. We also see that $(1,0)$ is a saddle when $\beta_2 < 1$, and an attractor when $\beta_2 > 1$. Similarly, $(0,1)$ is a saddle when $\beta_1 < 1$, and an attractor when $\beta_1 > 0$. To determine the stability of the coexistence fixed point, we check the sign of the trace and determinant of the Jacobian matrix:

$$\text{trace}(J_{(M_c^*,N_c^*)}) = \frac{1-\beta_1+\rho(1-\beta_2)}{\beta_1\beta_2-1}, \qquad \det(J_{(M_c^*,N_c^*)}) = -\frac{\rho(1-\beta_1)(1-\beta_2)}{\beta_1\beta_2-1}.$$

Hence, since β_1 and β_2 are both positive constants, $\beta_1, \beta_2 < 1$ implies that $\text{trace}(J_{(M_c^*,N_c^*)}) < 0$ and $\det(J_{(M_c^*,N_c^*)}) > 0$, making (M_c^*, N_c^*) an attractor. And similarly, $\beta_1, \beta_2 > 1$ implies that $\text{trace}(J_{(M_c^*,N_c^*)}) > 0$ and $\det(J_{(M_c^*,N_c^*)}) < 0$, making (M_c^*, N_c^*) a repeller. These four cases are summarized by the plots below.

4.2 A Two-Strain Treatment Model

We now turn to investigating the effects of incorporating a treatment term into the two-equation competition model. We propose the following model:

$$\frac{dx}{dt} = r_x x\left(1-\frac{x}{K_1}\right) - b_1xy - c_1x$$
$$\frac{dy}{dt} = r_y y\left(1-\frac{y}{K_2}\right) - b_2xy - c_2y,$$

Case 1: $\beta_1 < 1,\ \beta_2 < 1$

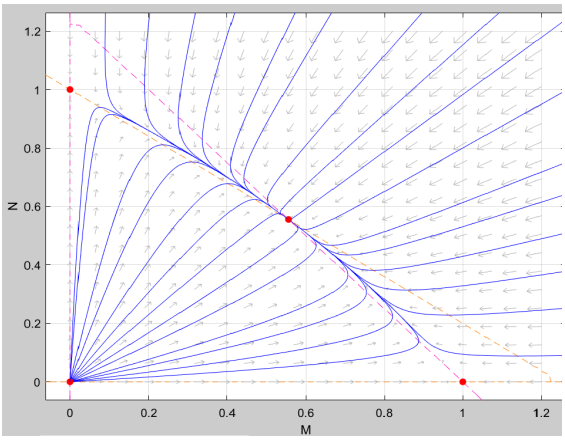

Fig 2.1: When $\beta_1, \beta_2 < 1$, the interspecies competition is low and the coexistence fixed point is attracting. The basin of attraction is almost the entire first quadrant.

Case 2: $\beta_1 > 1,\ \beta_2 > 1$

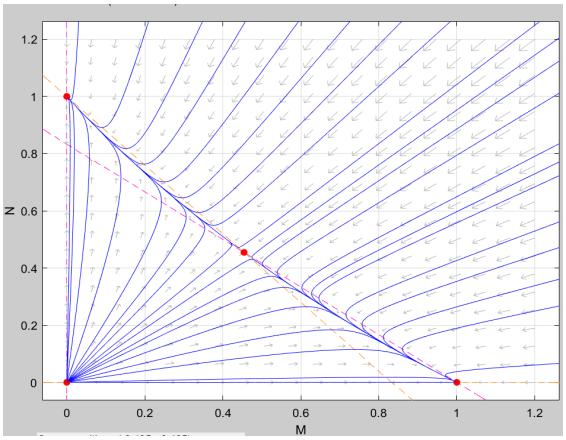

Fig 2.2: Interspecies competition his high, leading to competitive exclusion. The species that wins depends on the initial conditions.

Case 3: $\beta_1 < 1,\ \beta_2 > 1$

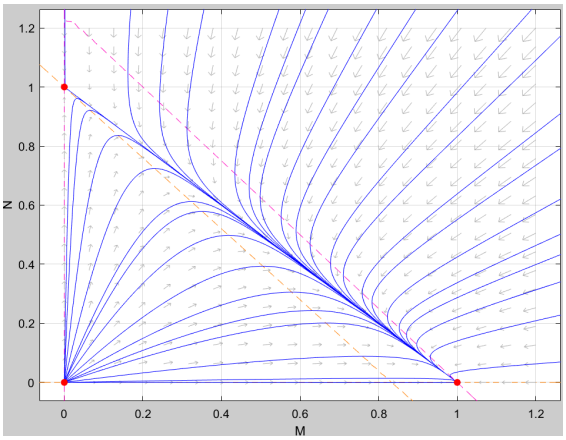

Fig 2.3: The competitive effect of x on y is stronger the competitive effect of y on x leading to competitive exclusion; y is driven to extinction for nearly all initial values.

Case 4: $\beta_1 > 1,\ \beta_2 < 1$

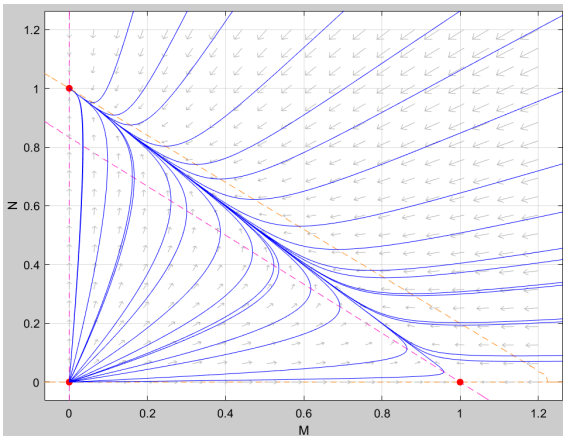

Fig 2.4: The competitive effect of y on x is stronger the competitive effect of x on y leading to competitive exclusion; x is driven to extinction for nearly all initial values.

where $c_1 x$ and $c_2 y$ are the treatment terms. The underlying assumption of the treatment model is that the cancer cell growth rate decreases in direct proportion to the concentration of a drug, which is assumed to be constant in time. The parameters c_1 and c_2 are positive constants proportional to the concentration of the drug. The non-dimensionalized model is given by

$$\frac{dM}{d\tau} = M(1 - M - \beta_1 N) - \delta_1 M$$
$$\frac{dN}{d\tau} = \rho N(1 - N - \beta_2 M) - \delta_2 N,$$

where $\delta_1 := c_1/r_x$ and $\delta_2 := c_2/r_y$ are nonnegative dimensionless parameters. This model has four fixed-points:

$$(0,0), (1-\delta_1, 0), (0, 1-\delta_2/\rho), \left(\frac{\beta_1(1-\frac{\delta_2}{\rho})+\delta_1-1}{\beta_1\beta_2-1}, \frac{\beta_2(1-\delta_1)+\frac{\delta_2}{\rho}-1}{\beta_1\beta_2-1}\right).$$

Then the Jacobian matrix evaluated at the generic fixed point (M^*, N^*) is

$$J_{(M^*,N^*)} = \begin{pmatrix} 1-2M^*-\beta_1 N^*-\delta_1 & -\beta_1 M^* \\ -\rho\beta_2 N^* & \rho(1-2N^*-\beta_2 M^*)-\delta_2 \end{pmatrix}.$$

For the first fixed point, the Jacobian matrix is

$$J_{(0,0)} = \begin{pmatrix} 1-\delta_1 & 0 \\ 0 & \rho-\delta_2 \end{pmatrix}$$

The eigenvalues are $1-\delta_1$ and $\rho-\delta_2$. Hence, $(0,0)$ is an attractor if and only if $\delta_1 > 1$ and $\delta_2 > \rho$. For the fixed point $(1-\delta_1, 0)$, the Jacobian matrix is

$$J_{(1-\delta_1,0)} = \begin{pmatrix} \delta_1-1 & \beta_1(\delta_1-1) \\ 0 & \rho+\rho\beta_2(\delta_1-1)-\delta_2 \end{pmatrix},$$

which has eigenvalues $\delta_1 - 1$ and $\rho+\rho\beta_2(\delta_1-1)-\delta_2$. Hence, $(1-\delta_1, 0)$ is stable if and only if $\delta_1 < 1$ and $\delta_2 > \rho+\rho\beta_2(\delta_1-1)$. A sufficient condition for stability is $\delta_1 < 1$ and $\delta_2 > \rho$. For the fixed point $(0, 1-\delta_2/\rho)$, the Jacobian matrix is

$$J_{(0,1-\delta_2/\rho)} = \begin{pmatrix} \beta_1(\frac{\delta_2}{\rho}-1)-\delta_1+1 & 0 \\ -\rho\beta_2(1-\frac{\delta_2}{\rho}) & \delta_2-\rho \end{pmatrix},$$

The eigenvalues are $\delta_2-\rho$ and $\beta_1(\frac{\delta_2}{\rho}-1)-\delta_1+1$. Hence, $(0, 1-\delta_2/\rho)$ is stable if and only if $\delta_2 < \rho$ and $\delta_1 > \beta_1(\delta_2/\rho-1)+1$. A sufficient condition for stability is $\delta_2 < \rho$ and $\delta_1 > 1$. And finally, the Jacobian matrix evaluated at the coexistence fixed point is

$$J_{co} = \begin{pmatrix} -M^* & -\beta_1 M^* \\ -\rho\beta_2 N^* & -\rho N^* \end{pmatrix},$$

where (M^*, N^*) denotes the coexistence fixed point. The stability is determined by the sign of the trace and determinant. We have

$$\text{Trace}(J_{co}) = -M^* - \rho N^*, \qquad \det(J_{co}) = \rho M^* N^* (1 - \beta_1 \beta_2).$$

Clearly the trace will always be negative (assuming the coexistence fixed point lies in the first quadrant). Therefore, the coexistence fixed point is stable if and only if $\det(J_{co}) < 0$, which occurs if and only if $\beta_1 \beta_2 < 1$.

Treatment Model Phase Portraits

$\rho = 0.5, \beta_1 = 0.4, \beta_2 = 0.3, \delta_1 = 0.5, \delta_2 = 0.3$

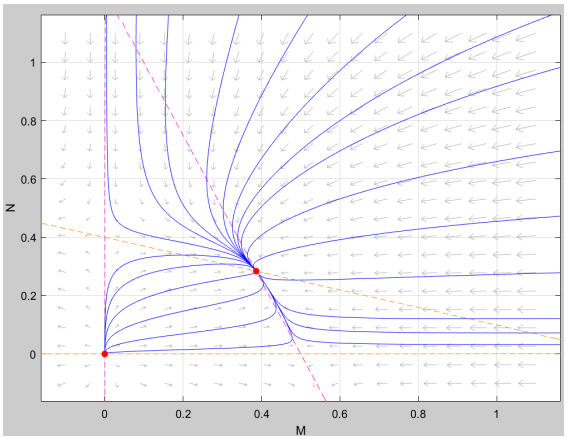

Fig 2.1: Interspecies competition is low and the intrinsic growth rate of y is small compared to that of x. Treatment effect is biased in favor of y. We see that all trajectories in interior of first quadrant tend towards the coexistence point.

$\rho = 1.2, \beta_1 = 1.5, \beta_2 = 0.99, \delta_1 = 0.01, \delta_2 = 0.2.$

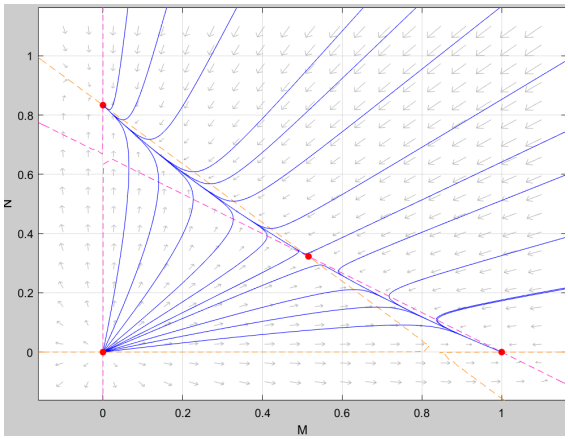

Fig 2.2: Interspecies competition favors y, and the intrinsic growth rate of y is higher than for x. A modest treatment effect targets y exclusively. Competitive exclusion is observed; the species that ultimately wins depends on the initial conditions.

$\rho = 1.5, \beta_1 = 0.9, \beta_2 = 1.5, \delta_1 = 0.2, \delta_2 = 1.6.$

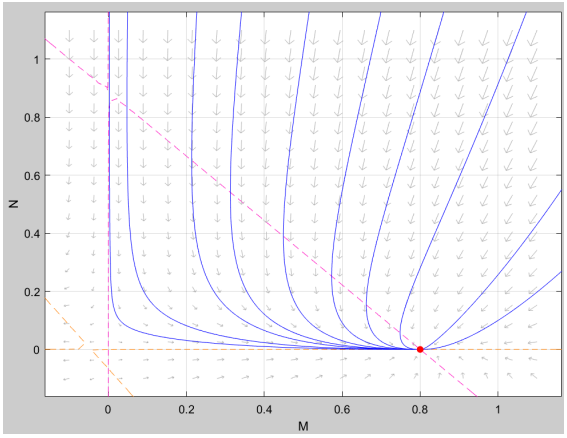

Fig 2.3: The competitive effect of x on y is stronger the competitive effect of y on x, while the intrinsic growth rate of y is greater than it is for x. Treatment is significantly biased against y. We observe competitive exclusion; y is driven to extinction for nearly all initial values.

$\rho = 1.5, \beta_1 = 0.9, \beta_2 = 1.5, \delta_1 = 1.1, \delta_2 = 0.7.$

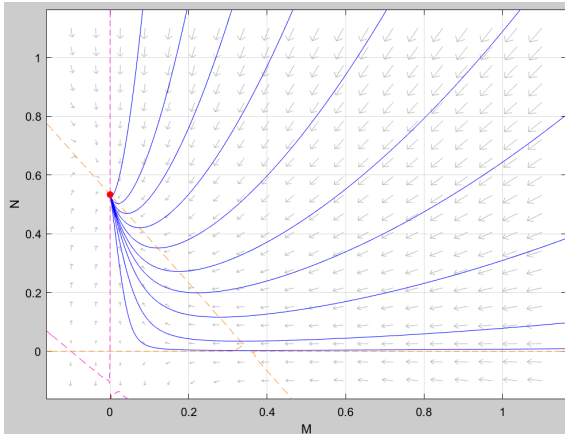

Fig 2.4: The competitive effect of x on y is stronger the competitive effect of y on x, while the intrinsic growth rate of y is larger than for x. Treatment is biased in favor of y, leading to competitive exclusion; x is driven to extinction for nearly all initial values.

5 Conclusion

In this project we analyzed tumor growth from statistical, machine learning, and differential equation perspectives. In our statistical approach, we fit the the Exponential, Power Law, and Gompertz-Laird models to tumor volume data in mice. We found that the Power Law model had the best fit and also the best predictive ability. This challenged our initial assumption that the Gompertz-Laird model, the most sophisticated of the three, would have the best fit. A possible explanation for this observation is that the sampling period of the data was too short, obscuring a possible limiting value or a leveling off in the growth rate. In light of the short sampling period, one might be led to believe that the exponential model would perform well, but this was not the case. Thus, the assumption that the relative tumor growth rate is constant in the early stages of growth is not well-supported. The strong performance of the Power Law with $\beta \approx 3/4$ may be indicative of a biological scaling law. As noted earlier, an allometric scaling argument has been made for $\beta = 2/3$ by considering the tumor as a sphere. Of course, this idealized assumption does not hold up in reality; tumors are never perfectly symmetrical and come in a variety of different shapes. Since the sphere is the shape which maximizes volume for a fixed surface area, a more oblong shape would in theory lend to a more favorable surface area to volume ratio (for the purposes of cells' access to nutrients). Hence, it makes sense that the optimal value for β in the Power Law model would be greater than 2/3.

We employed a Support Vector Regression model as a second approach. Unfortunately, the testing data it yielded was not a faithful predictor of the actual data. This does not come as a surprise given the paucity of training data that was used; machine learning algorithms such as SVR typically require very large amounts of training data to perform effectively. Another downside of the SVR model in this case is that it has less potential to furnish insight into biological principles, unlike the previous three models which are based on assumptions of tumor growth principles.

Lastly, we considered a slight variation of the competitive Lotka-Volterra equations which we modified with treatment terms. Compared to the previous two approaches we took, our results in this section are more theoretical, as we did not obtain data on healthy cells. We showed that there exist four qualitatively different scenarios for the competing populations

(which look almost identical to the scenarios of the original competitive Lotka-Volterra model) and we found stability conditions for each. The conditions for the stability of the cancer-extinction fixed point $(1 - \delta_1, 0)$ is probably of most practical interest. Our finding that $\delta_1 < 1$ and $\delta_2 > \rho + \rho\beta_2(\delta_1 - 1)$ gives a sense of the necessary degree and selectivity of treatment required for cancer eradication. We see that if the treatment targets the healthy cells beyond a certain threshold, eradication will not occur. Also, the larger the value of ρ, the greater the treatment effect on the cancerous cells must be to eradicate them. Unfortunately, the treatment model suffers from the unrealistic assumption that the population of cancerous and healthy cells are well-mixed. This assumption is of course not accurate because only the surface area of the tumors would be in contact with healthy cells. The biggest drawback of the Lotka-Volterra treatment model is the lack of data that is needed to validate it. Hence, our theoretical results should be taken with a grain (perhaps a lump) of salt.

One possible extension of this work would be to develop PDE equations in order to model the spatial dynamics of cancer growth. In our project, we neglected the aspect of spatial dynamics which was a significant shortcoming. We could then try to validate such a model using tumor imaging data. Another possibility would be to explore the dynamics between competing cancer strains or "quasispecies" possessing different degrees of fitness, and maybe also attempt to formulate and solve an optimal treatment strategy problem. Most importantly, in any future extension of our work we would make sure to obtain a much larger data set, as our lack of data was a major limitation of our project.

References

[1] K. Cronin, A. Lake, S. Scott, et al. Cancer statistics, 2019. *CA: A Cancer Journal for Clinicians*, 2019.

[2] A. K. Laird. Dynamics of tumor growth: Comparison of growth rates and extrapolation of growth curve to one cell. 1965.

[3] Spyridon Patmanidis, Alexandros C. Charalampidis, and Etc Al. Tumor growth modeling: Parameter estimation with maximum likelihood methods. *Computer Methods and Programs in Biomedicine*, 160:1–10, 2018.

[4] Rebecca L Siegel, Kimberly D Miller, and Ahmedin Jemal. Cancer statistics, 2019. *CA: A Cancer Journal for Clinicians*, 2019.

[5] Kathleen M. C. Tjorve and Evan Tjorve. The use of gompertz models in growth analyses, and new gompertz-model approach: An addition tohe unified-richards family. 2017.

[6] Peter J Wangersky. Lotka-volterra population models. *Annual Review of Ecology and Systematics*, 9:189–218, 1978.

[7] Dominik Wodarz and Natalia Komarova. *Dynamics of Cancer: Mathematical Foundations of Oncology*. WSPC, Hackensack, NJ, 2014.